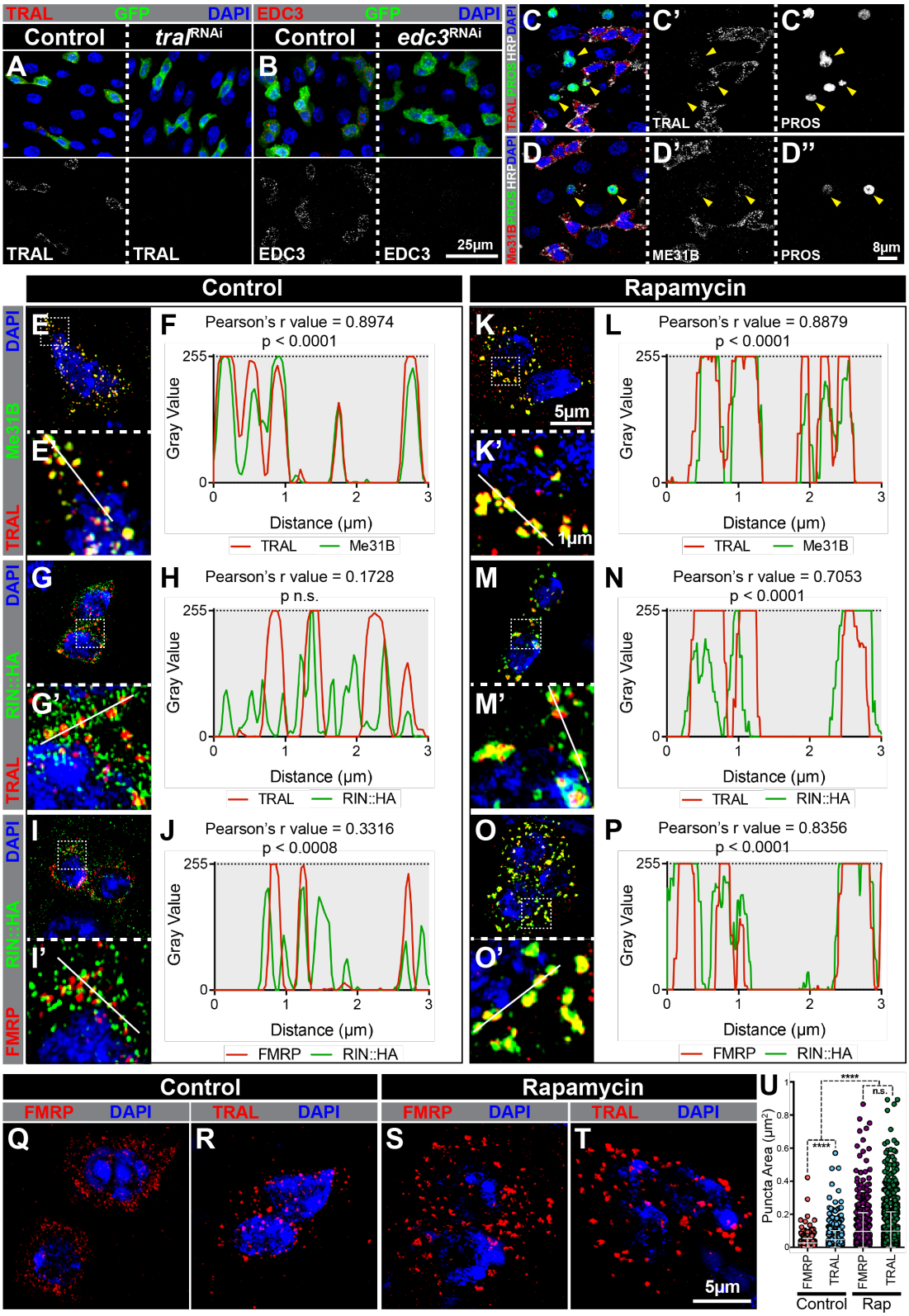

Figure S1. Comparative analysis of P-body and stress granule component expression, Related to Figure 1.

(A-B) Progenitor cells from (A) *esg*^{TS} (control, left), *esg*^{TS} */ tral* RNAi (right) or (B) *esg*^{TS} (control, left), *esg*^{TS} */ edc3* RNAi (right) intestines stained for (A) TRAL (red) or (B) EDC3 (red). Note that *tral* or *edc3* mutant GFP+ intestinal progenitors have no detectable TRAL or EDC3 staining, respectively. (C-D) Confocal micrographs of intestinal sections stained for (C) TRAL (red) or (D) Me31B (red), (C-D) PROS (green), (C-D) HRP (white) and (C-D) DAPI. While TRAL and Me31B granules are readily observed in all HRP+ intestinal progenitors, only some Prospero+ EEs have detectable TRAL or Me31B expression. (E, G, I, K, M, O) Super-resolution micrographs of progenitor cells treated with either (E, G, I) KRB or (K, M, O) 1mM rapamycin in KRB and stained for (E, K) TRAL (red), Me31B (green) or (G, M) TRAL (red), RIN::HA (green) or (I, O) FMRP (red), RIN::HA (green) and DAPI (blue in E, G, I, K, M, O). E', G', I', K', M', and O' show a magnified view of the region marked with white dotted outline in E, G, I, K, M, and O respectively. (F, H, J, L, N, P) Line plots of fluorescent intensity profiles of (F, L) TRAL (red), Me31B (green) or (H, N) TRAL (red), RIN::HA (green) or (J, P) FMRP (red), RIN::HA (green). The plot shows the pixel-by-pixel gray value of each channel along white lines in E', G', I', K', M' or O'. Computed Pearson's r value and the statistical significance of the correlation are given above each plot. Note that Me31B and TRAL are P-body proteins while FMRP and RIN::HA are stress granule proteins. (Q-T) Super-resolution micrographs of progenitor cells treated with either (Q-R) KRB (control) or (S-T) 1mM rapamycin in KRB, and stained for (Q, S) FMRP (red) or (R, T) TRAL (red) and (Q-R) DAPI (blue). (U) Scatter dot plots of FMRP or TRAL puncta area in progenitor cells treated with control (n=629 or 657) or 1mM rapamycin (n=804 or 1215) in KRB. Error bars on plots show mean±s.d. and asterisks denote statistical significance from Kruskal-Wallis test (l) $^{**}p < 0.01$; $^{****}p < 0.0001$; n.s., not significant.

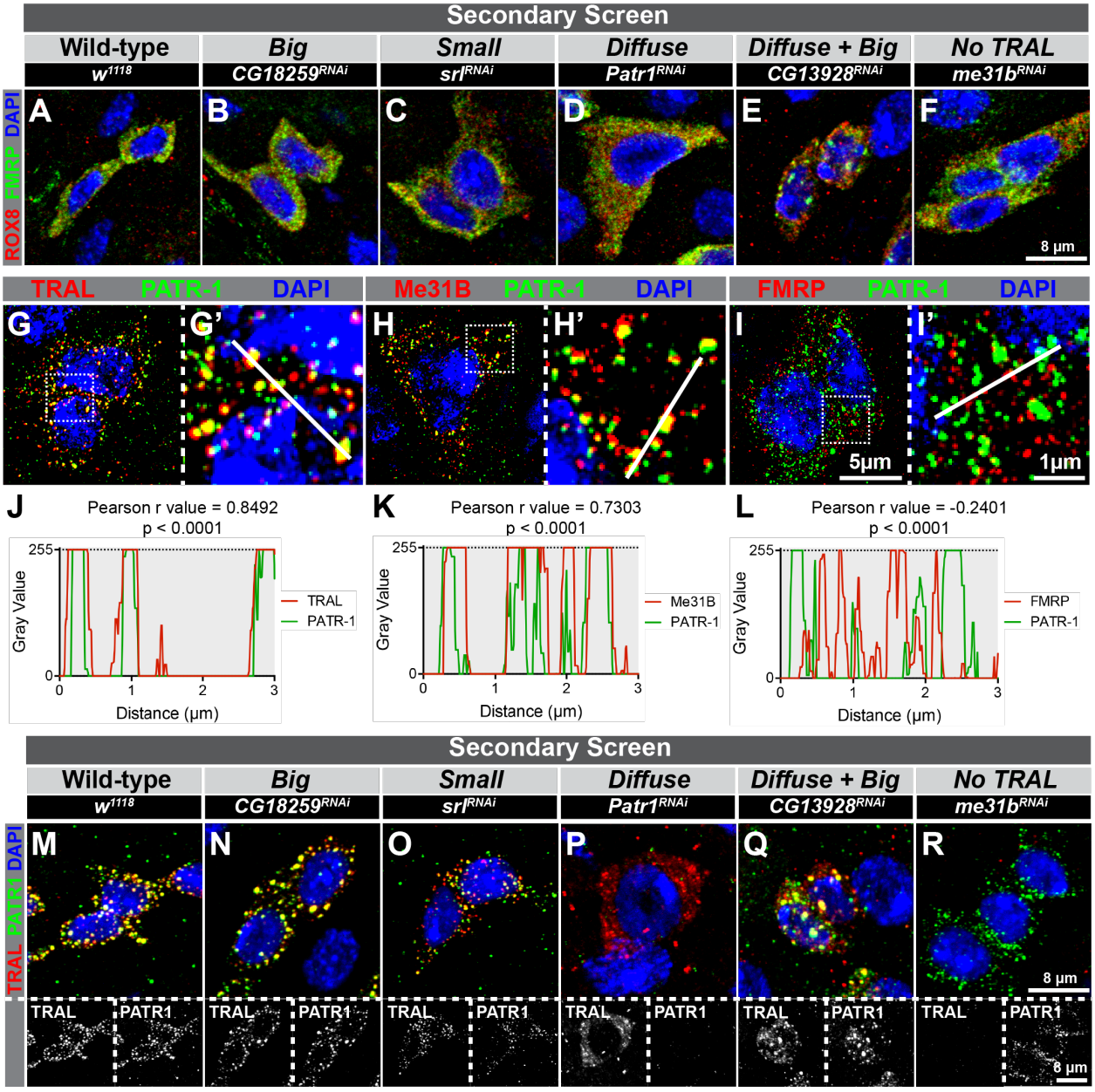

Figure S2. A targeted genetic screen identifies genes affecting P-body morphology including the P-body component PATR-1, Related to Figure 2.

(A-F) Confocal micrographs of intestinal progenitors from (A) *esg*^{TS}, (B) *esg*^{TS} / *CG18259* RNAi, (C) *esg*^{TS} / *srl* RNAi, (D) *esg*^{TS} / *Patr-1* RNAi, (E) *esg*^{TS} / *CG13928* RNAi or (F) *esg*^{TS} / *me31b* RNAi posterior midguts and stained for ROX8 (red), FMRP (green) and DAPI (blue). (G-I) Super-resolution micrographs of intestinal progenitors stained for (G-G') TRAL (red), PATR-1 (green) or (H-H') Me31B (red), PATR-1 (green) or (I-I') FMRP (red), PATR-1 (green) and DAPI (blue in G-I and G'-I'). (J-L) Line plots

showing fluorescent intensity profiles of (J) TRAL (red) or (K) Me31B (red) or (L) FMRP (red) and PATR-1 (green). The plot shows the normalized pixel-by-pixel gray value of each channel along white lines shown on G'-I'. Computed Pearson's r values and the statistical significance of the correlation are given above each plot. (M-R) Confocal micrographs of intestinal progenitors from (M) esg^{TS}, (N) esg^{TS} / *CG18259* RNAi, (O) esg^{TS} / *srl* RNAi, (P) esg^{TS} / *Patr-1* RNAi, (Q) esg^{TS} / *CG13928* RNAi or (R) esg^{TS} / *me31b* RNAi posterior midguts and stained for TRAL (red), PATR-1 (green) and DAPI (blue). Gray-scale images of TRAL and PATR-1 in panels are shown below the respective panel.

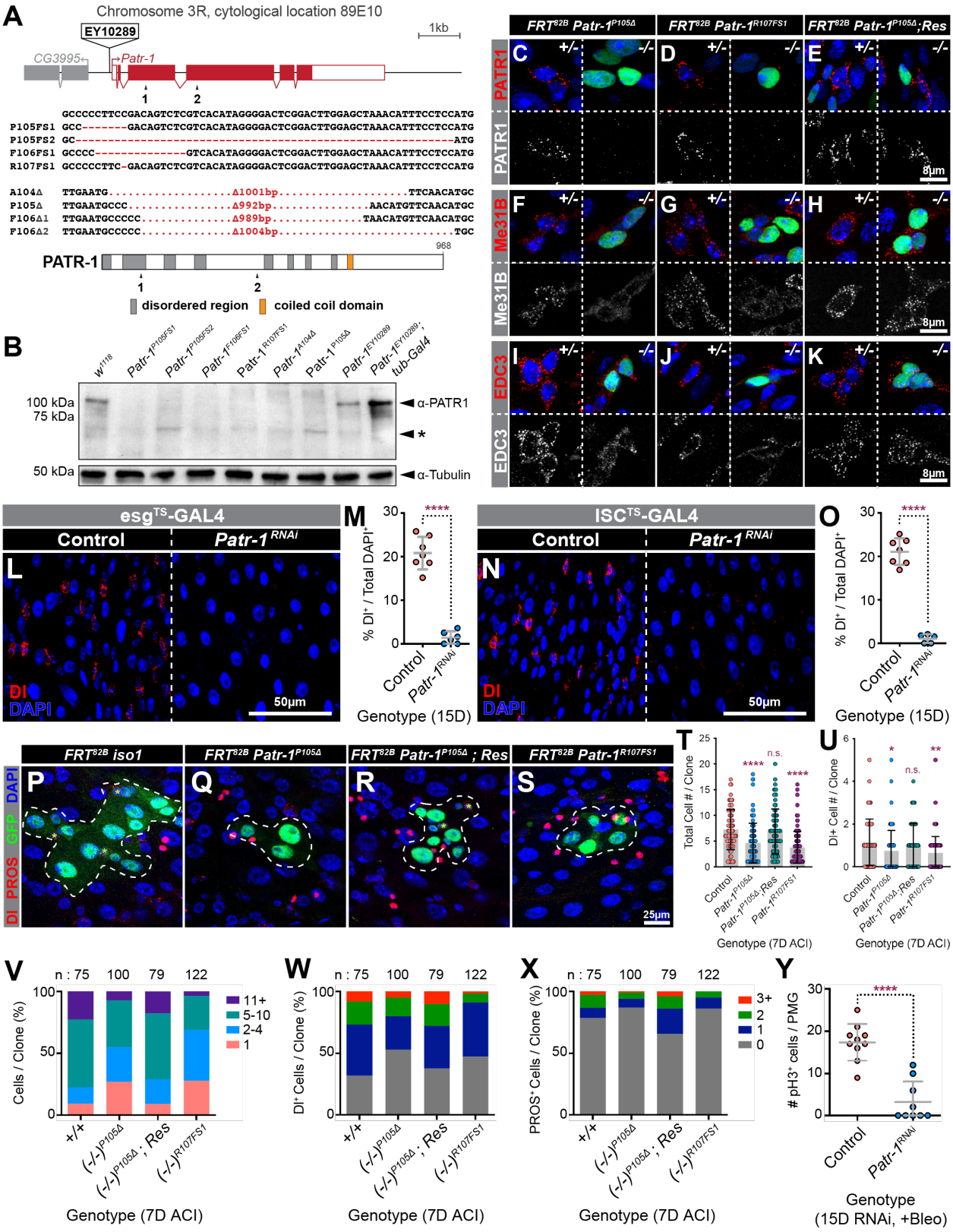

Figure S3. Loss of *Patr-1* blocks P-body formation, reduces the number of ISCs, and total number of cells per clone, Related to Figure 3.

(A) Schematics of the *Patr-1* locus and PATR-1 protein showing the locations of the two gRNAs (arrowheads) used to generate new alleles as well as the nucleotide changes associated with these alleles. (B) Western blot of w^{1118} (control), *Patr-1* mutant, and $Patr1^{EY10289}$ / *tub-GAL4* larval extracts probed with anti-PATR-1 (top panel) or Tubulin (bottom panel) antibodies. A prominent background band detected by the PATR-1 antibody is labeled (*). (C-K) MARCM-labeled homozygous mutant (right, -/-) and neighboring unlabeled heterozygous (left, +/-) $Patr\text{-}1^{P105\Delta}$ (C, F, I), $Patr\text{-}1^{R107FS1}$ (D, G, J), or rescued $Patr\text{-}1^{P105\Delta}$ (E, H, K) progenitor cells stained for GFP (green), DAPI (blue) and either PATR-1 (red in C-E), Me31B (red in F-H) or EDC3 (red in I-K). (L) Sections from esg^{TS} (left) or esg^{TS} / *Patr-1* RNAi (right) midguts after 15 days at 29°C stained for Dl (Delta, red), and DAPI (blue). (M) Dot-plot showing the percentage of ISCs marked by Dl staining (n=5) of indicated genotypes after 15 days at 29°C. (N) Sections from *ISC-KCKT-GAL4*^{TS} (left) or *ISC-KCKT-GAL4*^{TS} / *Patr-1* RNAi (right) 15 days after shifting to 29°C and stained for Dl (red) and DAPI (blue). (O) Dot-plot showing the percentage of ISCs marked by Dl staining (n=5) of indicated genotypes after 15 days at 29°C. (P-S) Representative confocal images of *tub-Gal4, UAS-GFP*-labeled (P) control, (Q) $Patr\text{-}1^{P105\Delta}$, (R) rescued $Patr\text{-}1^{P105\Delta}$, or (S) $Patr\text{-}1^{R107FS1}$ homozygous clones stained for Dl (red), PROS (red), GFP (green) and DAPI (blue). The size of the clone is marked by the white dotted line and ISCs in clones are denoted by the yellow asterisks (*). (T-U) Dot-plot showing the (T) total cell or (U) Dl+ ISC number per *tub-Gal4, UAS-GFP*-labeled control, $Patr\text{-}1^{P105\Delta}$, rescued $Patr\text{-}1^{P105\Delta}$, or $Patr\text{-}1^{R107FS1}$ homozygous clones analyzed 7 days after clone induction (ACI). (V-X) Binned bar plots showing the quantification of (V) total cell, (W) Dl+ ISC or (X) PROS+ EE cell numbers in *tub-Gal4, UAS-GFP*-labeled control, $Patr\text{-}1^{P105\Delta}$, rescued $Patr\text{-}1^{P105\Delta}$, or $Patr\text{-}1^{R107FS1}$ homozygous clones analyzed 7 days ACI. Note that n indicates the total number of clones analyzed for each genotype. Rescued (Res) strains harbor the *Patr-1* rescuing transgene, *P21M20*. (Y) Dot-plot showing the total number of pH3+ mitotic cells per posterior midgut of esg^{TS} (n=10) or esg^{TS} / *Patr-1* RNAi (n=9) flies fed with bleomycin for 24 hours. Error bars on plots show mean±s.d. and asterisks denote statistical significance from Unpaired t-test (M, O, Y), or Kruskal-Wallis test (T-U). *$p < 0.05$; **$p < 0.01$; ****$p < 0.0001$; n.s., not significant.

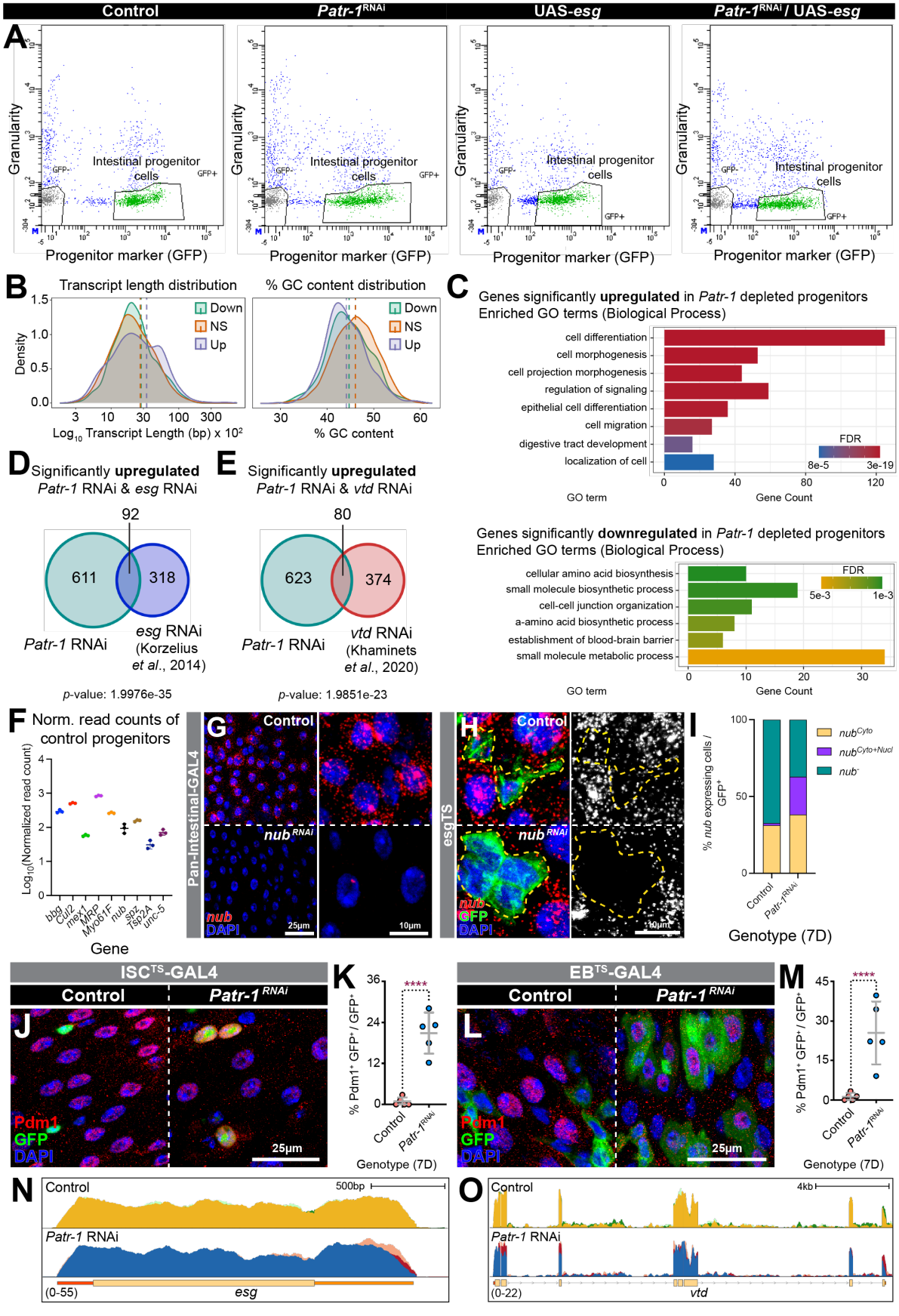
Control
Patr-1RNAi
UAS-esg
Patr-1RNAi / UAS-esg
A
Granularity
Intestinal progenitor cells
GFP-
GFP+
Progenitor marker (GFP)
B
Transcript length distribution
% GC content distribution
Down
NS
Up
Density
Log10 Transcript Length (bp) x 10^2
% GC content
C
Genes significantly upregulated in Patr-1 depleted progenitors
Enriched GO terms (Biological Process)
cell differentiation
cell morphogenesis
cell projection morphogenesis
regulation of signaling
epithelial cell differentiation
cell migration
digestive tract development
localization of cell
FDR
8e-5
3e-19
GO term
Gene Count
Genes significantly downregulated in Patr-1 depleted progenitors
Enriched GO terms (Biological Process)
cellular amino acid biosynthesis
small molecule biosynthetic process
cell-cell junction organization
a-amino acid biosynthetic process
establishment of blood-brain barrier
small molecule metabolic process
5e-3
1e-3
D
Significantly upregulated
Patr-1 RNAi & esg RNAi
92
611
318
Patr-1 RNAi
esg RNAi (Korzelius et al., 2014)
p-value: 1.9976e-35
E
Significantly upregulated
Patr-1 RNAi & vtd RNAi
80
623
374
Patr-1 RNAi
vtd RNAi (Khaminets et al., 2020)
p-value: 1.9851e-23
F
Norm. read counts of control progenitors
Log10(Normalized read count)
bbg
Cul2
mex1
MRP
Myo61F
nub
spz
Tsp2A
unc-5
Gene
G
Control
Pan-Intestinal-GAL4
nubRNAi
nub
DAPI
25µm
10µm
H
Control
esgTS
nubRNAi
nub
GFP
DAPI
10µm
I
% nub expressing cells / GFP+
nubCyto
nubCyto+Nucl
nub-
Control
Patr-1RNAi
Genotype (7D)
ISCTS-GAL4
Control
Patr-1 RNAi
J
Pdm1
GFP
DAPI
25µm
K
% Pdm1+ GFP+ / GFP+
****
Control
Patr-1RNAi
Genotype (7D)
EBTS-GAL4
Control
Patr-1 RNAi
L
Pdm1
GFP
DAPI
25µm
M
% Pdm1+ GFP+ / GFP+
****
Control
Patr-1RNAi
Genotype (7D)
N
Control
500bp
Patr-1 RNAi
(0-55)
esg
O
Control
4kb
Patr-1 RNAi
(0-22)
vtd

Figure S4. Gene expression changes associated with *Patr-1* RNAi, Related to Figure 4.

(A) FACS profiles of *esg^{TS}*, *esg^{TS} / Patr-1 RNAi*, *esg^{TS} / UAS-esg*, and *esg^{TS} / Patr-1 RNAi* / *UAS-esg* intestines. (B) Density plot showing the $\log_{10}$ transcript length distribution or % GC content of significantly upregulated (Up, purple), downregulated (Down, green) or unchanged (NS, orange) genes. (C) Bar plot showing a selected set of significantly enriched Gene Ontology (GO) terms for genes that are significantly upregulated or downregulated in *Patr-1* RNAi compared to control. (D-E) Venn diagrams of overlap between significantly upregulated genes in *Patr-1* RNAi and (D) *esg* RNAi [53], or (E) *vtd* RNAi [52]. Note that datasets from Korzelius et al., 2014 and Khaminets et al., 2020 were reanalyzed with *Patr-1* RNAi using the in-house analysis pipeline. (F) Dot plot showing the log normalized read counts of a selected set of pro-differentiation genes in wildtype intestinal progenitor cells based on the transcriptomic experiment. (G) Sections from *Pan-Intestinal-GAL4^{TS}* (left) or *Pan-Intestinal-GAL4^{TS} / nub* RNAi (right) midguts after 7 days at 29°C stained for *nub* mRNA (red) and DAPI (blue). (H) Fluorescent micrographs of *esg^{TS}* and *esg^{TS} / Patr-1* RNAi midguts after 7 days at 29°C and stained for *nub* mRNA (red), GFP (green), and DAPI (blue). (I) Binned bar plots showing the quantification of percentage of progenitor cells with no (*nub^{-}* in green), only cytoplasmic (*nub^{Cyto}* in yellow) or cytoplasmic + nuclear (*nub$^{Cyto+Nucl}$* in purple) *nub* staining. (J) Sections from *ISC-KCKT-GAL4^{TS}* (left) or *ISC-KCKT-GAL4^{TS} / Patr-1* RNAi (right) midguts after 7 days at 29°C stained for Pdm1 (red), GFP (green) and DAPI (blue). Note that GFP labels ISCs of the intestinal epithelium. (K) Dot-plot showing the percentage of ISCs with nuclear Pdm1 staining (n=5) of indicated genotypes after 7 days at 29°C. (L) Sections from *gbe^{TS}* (left) or *gbe^{TS} / Patr-1* RNAi (right) 7 days after shifting to 29°C and stained for Pdm1 (red), GFP (green) and DAPI (blue). Note that GFP labels EBs of the intestinal epithelium. (M) Dot-plot showing the percentage of EBs with nuclear Pdm1 staining (n=5) of indicated genotypes after 7 days at 29°C. (N-O) Genome browser tracks of CPM-normalized control and *Patr-1* RNAi at the (N) *esg* and (O) *vtd* loci. Note the three replicates of the control (yellow, light green and dark green) and the three replicates of the *Patr-1* RNAi (blue, pink and red) on N-O,

have been overlayed for simplicity. Error bars on plots show mean±s.d. and asterisks denote statistical significance from Unpaired t-test (K, M). ****$p < 0.0001$.

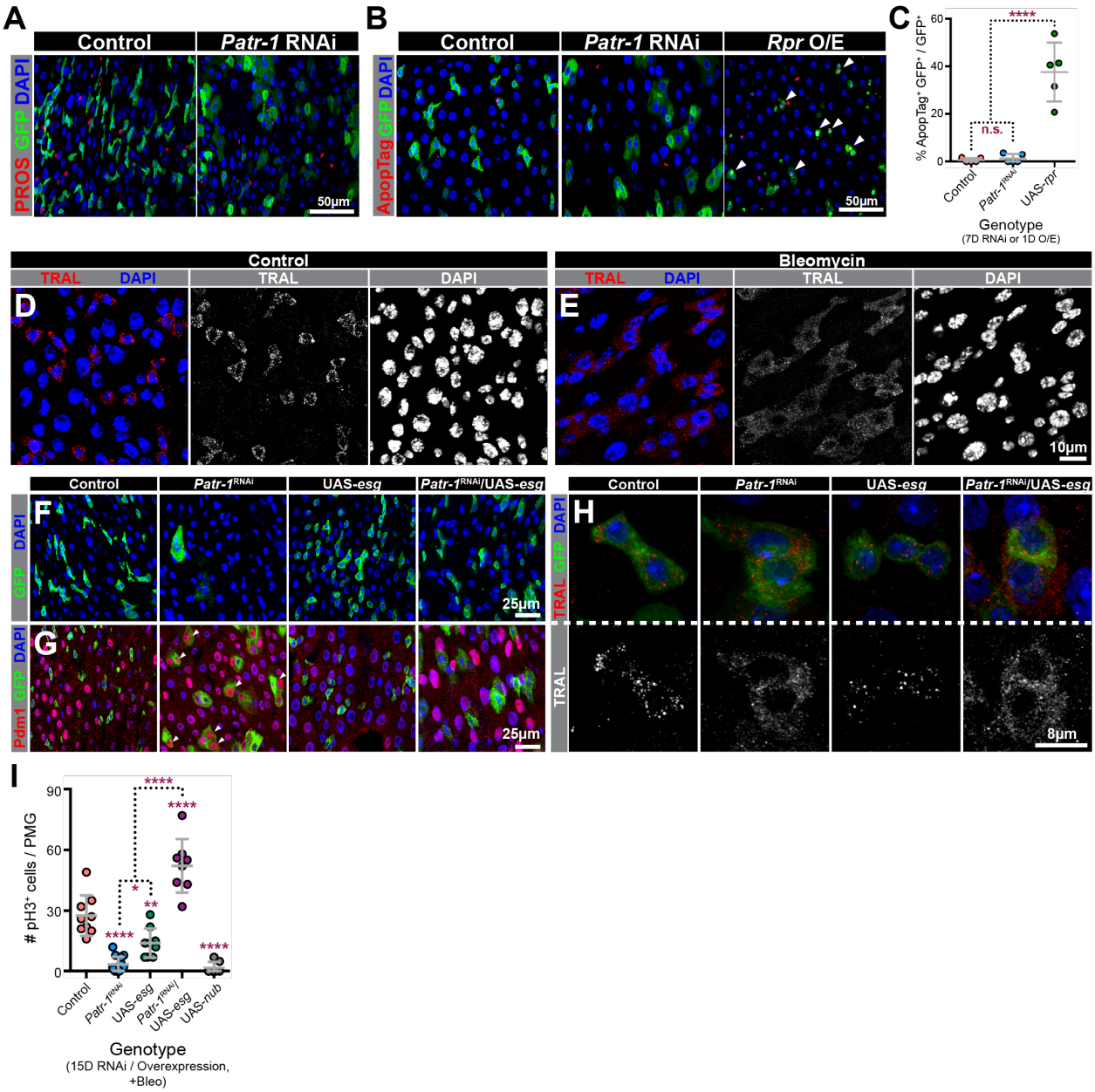

Figure S5. *Patr-1* RNAi does not lead to an increase in the number of EEs or the amount of cell death, Related to Figure 5.

(A-B) Confocal micrographs of intestinal sections from (A) *esg*^{TS} and *esg*^{TS} / *Patr-1* RNAi or (B) *esg*^{TS}, *esg*^{TS} / *Patr-1* RNAi and *esg*^{TS} / UAS-*rpr* and stained for (A) PROS (red) or (B) ApopTag (red) and GFP (green) and DAPI (blue). White arrowheads on B show ApopTag^{+} GFP^{+} cells in the field. (C) Plot of normalized ApopTag^{+} progenitor cells in *esg*^{TS} (n=5), *esg*^{TS} / *Patr-1* RNAi (n=5), and *esg*^{TS} / *UAS-rpr* (n=5) midguts after 7 days of RNAi or 1 day of *rpr* overexpression at 29ºC. (D-E) Fluorescent micrographs of

intestinal sections from w1118 flies fed with (D) 5% sucrose in water (control) or (E) 5% sucrose and 25 µg/ml bleomycin in water (bleomycin) and stained for TRAL (red) and DAPI (blue). (F-G) Sections from *esg^{TS}*, *esg^{TS} / Patr-1 RNAi*, *esg^{TS} / UAS-esg*, or *esg^{TS} / Patr-1 RNAi* / *UAS-esg* intestines stained for Pdm1 (red, only in G), GFP (green, F-G) and DAPI (blue, F-G). (H) Confocal micrographs of intestinal progenitors from *esg^{TS}*, *esg^{TS} / Patr-1* RNAi, *esg^{TS} / UAS-esg*, or *esg^{TS} / Patr-1 RNAi / UAS-esg* posterior midguts stained for TRAL (red), GFP (green) and DAPI (blue). (I) Bleomycin-induced pH3+ cell number per posterior midgut (n=9, 14, 9, 8, or 7) of indicated genotypes after 15 days at 29ºC. Error bars on plots show mean±s.d. and asterisks denote statistical significance from Ordinary one-way ANOVA with Turkey's multiple comparison test (C, I). ****$p < 0.0001$, n.s. = not significant.